IEEE Access
Multidisciplinary ⋮ Rapid Review ⋮ Open Access Journal

Received 4 July 2023, accepted 22 July 2023, date of publication 27 July 2023, date of current version 7 August 2023.

Digital Object Identifier 10.1109/ACCESS.2023.3299446

RESEARCH ARTICLE

Development of Hybrid-Actuator Robotic Exoskeleton Based on Gesture Signal Recognition Algorithm for the Rehabilitation of Dysfunctional Finger

SHIXIAN ZHAO[1], JINCAN LEI[1], QIHENG TIAN[1], ZHIHAO YANG[2], AND JING HUANG[1]

[1]Chongqing Engineering and Technology Research Center of Intelligent Rehabilitation and Eldercare, Chongqing City Management College, Chongqing 401331, China

[2]Key Laboratory for Biorheological Science and Technology of Ministry of Education, Bioengineering College, Chongqing University, Chongqing 400044, China

Corresponding author: Jincan Lei (458740894@qq.com)

This work was supported in part by the Science and Technology Research Program of Chongqing Municipal Education Commission under Grant KJQN202103308; in part by the Natural Science Foundation of Chongqing under Grant cstc2021jcyj-bsh0268; in part by the Research on the Teaching Reform of Higher Education in Chongqing under Grant Z213092; in part by the Project of Science and Technology Research Program of Chongqing Education Commission of China under Grant KJQN201903312; in part by the Scientific Research Foundation for High-Level Talents of Chongqing City Management College under Grant 2020kyqd01, Grant 2017kyqd01, and Grant 2017kyqd02; in part by the Research and Innovation Team Program of Chongqing City Management College under Grant KYTD202107; and in part by the Collaborative Innovation Team of Philosophy and Social Sciences.

ABSTRACT The present work, which describes the development of a novel, portable, low-cost, effective, hybrid-actuator rehabilitation exoskeleton, aims to present a solution for the rehabilitation of functional finger injuries. In this robotic system, a simple and ingenious actuator is designed on the synchronizing wheel of each finger joint, which enables the independent passive training of each finger joint with the actuation of the motor. In addition, three damping shafts with leaf springs as another type of actuator, corresponding to PIP, MIP and DIP joints, are used as damping devices to supply the damping force for active training. Moreover, a gesture-based signal recognition algorithm, including a preprocessing algorithm, a feature vector extraction algorithm, and a clustering algorithm, is designed and integrated to serve the system for further automatic controllability. By utilizing this hybrid actuator mode, the robotic exoskeleton is able to train each finger joint independently in a passive training mode and maintain the damping force output within acceptable ranges for different levels of muscle strength. Importantly, with further optimization and upgrades, we deduce that this system has excellent potential applications for finger rehabilitation.

INDEX TERMS Rehabilitation, signal processing, pattern recognition, stroke, robotics.

I. INTRODUCTION

In recent years, the incidence of stroke is gradually increasing around the world, which leads to stroke turning into the second cause of death and the third most significant source of disability [1], [2]. This current situation is inextricably related to hypertension [3], [4], [5], hyperlipidemia [6], [7], [8], the growth in the number of older people, and the decline in muscle strength and physical mobility of elderly people. Even when the patient's condition improves significantly with the help of modern medical technology, most stroke survivors suffer from various degrees of limb motor dysfunction. A major symptom of stroke is hemiplegia, a common sequelae of impaired movement of the limbs. It seriously reduces the quality of life for stroke survivors and places a significant financial burden on the families involved and the entire community. In particular, functional injury of the hand is one of the typical sequelae of stroke. Clinical medical studies have verified that a certain intensity of training can be effective in helping patients regain the use of their

The associate editor coordinating the review of this manuscript and approving it for publication was Santosh Kumar.

limbs. In addition, the ability to relearn in a functional area of the brain can be effectively enhanced, accompanied by rehabilitation of motor limb function; otherwise, there is an elevated potentiality to cause permanent function damage [9], [10], [11].

Up to now, finger rehabilitation training still adopts the ''one-on-one'' mode, which needs a doctor to take care of a patient. First, the doctor assesses the motor function of the damaged limb. Afterwards, an independent rehabilitation training program can be developed. Finally, various training movements can be performed accurately with the guidance and assistance of a physician. It is extremely traditional and costs plenty of medical resources. However, this mode has numerous shortcomings: First, the training efficiency and training intensity are considerably affected by the subjectivity of the rehabilitation physician, so the training effect primarily depends on the level and experience of the rehabilitation physician [12]. Second, the rehabilitation training mode of ''one on one'' is highly traditional and inefficient aiming at the ever-increasing aging population, which is likely to cause a large waste of medical resources [13]. Third, traditional rehabilitation training modalities do not accurately control and record training parameters such as speed, trajectory, and intensity, and it is difficult to quantify and objectively evaluate the training and rehabilitation effects. Fourth, it is also difficult to optimize the training parameters, which is not conducive to an in-depth study of the neural rehabilitation laws of patients. Finally, it is not conducive to the formulation of the best rehabilitation training programs.

In recent years, the development of robotics technology has received increasingly attention in rehabilitation training [1], [14], [15], [16]. Among them, the development and promotion of finger rehabilitation robots (FRRs) provides an effective way to break the limits of the above-mentioned treatment modes. August et al. [17] designed a finger telerehabilitation training system using P5 data gloves. The system uses data, gloves and specific games to perform rehabilitation training on the hand and monitor and analyze muscle movement function in real time. Thielbar et al. [18] designed a single-finger telerehabilitation training virtual reality system suitable for home rehabilitation training. The system can test and record flexion and extension of the fingers and wrists, allowing rehabilitation physicians to monitor patient training progress and communicate with patients while providing real-time assistance. Li et al. [19] reported fiber Bragg gratings (FBGs) embedded in silicone tubes for finger joint movement monitoring. This technology is incorporated in the finger rehabilitation robots, which can precisely control the finger rehabilitation movement of stroke patients. Golomb et al. [20] designed a virtual reality-based remote hand function rehabilitation therapy glove. This virtual glove can track and record hand movement trajectories on a webcam and perform data analysis. The system is simple in structure, powerful in versatility and low in cost. Although various finger robot rehabilitation functions have been created, the current situation is that there are still some unavoidable drawbacks limiting these FRRs to apply in research institutes and not suitable for home or community applications [21]. The common drawback of FRRs is that the mechanics are too simple for active training. Inconvenience of operation and cumbersome and costly instrumentation remain to be addressed. And the recovery effect is less pronounced, resulting in poor utility. Taking into account the demands of different stages of rehabilitation, the design requirement of FRRs is to be able to provide different training modes [22]. Commonly, the training modes are divided into two categories, active training and passive training [23], [24]. The passive training mode is appropriate for finger paralysis or spasticity. In this state, the fingers are unable to make any independent movement. Accordingly, the fingers are driven by the FRRs and complete the prescribed training actions, recovering the activity of the finger joints gradually. Accordingly, the fingers are driven by the FRRs and complete the prescribed training actions, gradually restoring the activity of the knuckles. Correspondingly, the other training mode is the active training mode, which is more appropriate for the recovery phase with a certain strength and range of motion of the fingers. The fingers are required to overcome a variety of resistance strengths while flexing or extending voluntarily throughout the training. This mode helps the muscles perform strength training and promotes the recovery of motor function in the fingers. Thus, the aim of this study is to develop a controllable, bi-modal and portable FRR to meet the needs of patients at various stages of recovery. In this design, a direct-current motor (DC motor) is applied to provide a bidirectional force for passive training. It is a common, stable, and easy to integrate type of actuator which appeared in the previous FRRs [25], [26], performing the transmission system. Active training was applied using a controllable damping shaft with leaf springs. It has a tiny size, easy installation, low cost, quick response, and excellent controllability. To improve the flexibility of passive training, an AI signal recognition algorithm (GRA) based on sEMG is put forward for gesture recognition, which can be used to analyze and train the acquired data for gesture classification. The proposed system is able to accurately perform independent training of all three knuckles.

II. EXPERIMENTAL SECTION

A. MECHANICAL DESIGN

A fully functional rehabilitation system for dysfunctional finger training is constructed and the mechanical structure of the system is shown in Figure 1. The system mainly consists of a parameter sensing subsystem, a control and transmission subsystem, an arm brace, a palm support component, and a data processing subsystem. Briefly, the sensing subsystem is responsible for the real-time monitoring and feedback of parameters such as force, angle, position, etc.. The control and transmission subsystem included a 32-Bit microcontroller (STM32F303 MCU purchased from ST semiconductor company) and its peripheral function circuits, a stepper motor and transmission belt. We used 3D printing technology

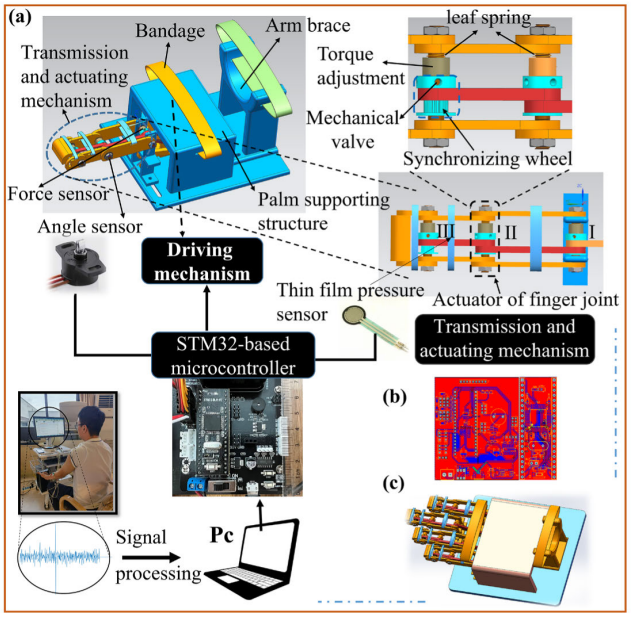

FIGURE 1. Illustration of the hybrid-actuator exoskeleton: (a) the flow direction of the black arrow is the process of passive control for single finger, (b) Circuit design of STM-32 based microcontroller, (c) the complete hybrid-actuator exoskeleton for four-fingers rehabilitation.

to make exoskeleton parts, which contained synchronizing wheels I, II, and III linked to the spindles of the proximal interphalangeal point (PIP), middle interphalangeal point (MIP), and distal interphalangeal point (DIP), respectively.

To run the whole system smoothly, the control and transmission subsystem controls the peripheral function modules through receiving instructions from the micro-computer ARM11 for resource allocation. The data processing subsystem processes the parameter data returned by the peripheral sensor devices. In addition, the palm training position is changed from down to up, allowing the entire palm to be placed on the supporting components to relieve the fatigue caused by the training process. To ensure that the remaining four fingers except the thumb can be trained as efficiently as possible, the size of the system should be reduced. Thus, depending on the different injured fingers of the patient, a chute is designed to change the position of the motion to improve the practicability of the system.

B. ACQUISITION MODALITY

The main component of the acquisition device is a Surface EMG (sEMG) Acquisition Wire-less Transmission System®, which consists of a base station and multichannel electrodes. The base station equipped with a self-contained rechargeable battery achieves a data transmission range of 100 m. The electrodes can simultaneously collect a maximum of 16 channels of surface myoelectric signals. These data are sampled at a rate of 3 kHz with a common mode rejection ratio of greater than 110 dB and a baseline noise of less than 0.4 μV (RMS). The base station transmits this data to the laptop responsible for data collection via a proprietary wireless communication protocol. After completing the collection of one set of gesture data from the experimenter, a short rest period is required for the second acquisition in the same way. Since the whole acquisition process is continuous, the collected data includes data from both resting and active states of the hand. Therefore, effective preprocessing has to be performed to obtain the sEMG signal corresponding to the gesture.

C. DATA ANALYSIS METHOD

There has been increasing interest in applying learning algorithms to process sEMG signals to improve the accuracy and dexterity of FRR in the passive training model [27], [28], [29]. To distinguish different types of gestures with multiple degrees of flexion of the finger joints, we use multiple processing steps such as denoising preprocessing, eigenvalue extraction, and feature vector reconstruction to precisely analyze the raw data. All original signals selected for classification research were obtained from the surface electromyography device, purchased from NCC Electronic Co., Ltd (Shanghai, China). In this work, there are eight gestures (flexion and extension of the ring finger, middle finger, index finger, and little finger), theoretically corresponding to eight kinds of EMG signals, each of which is preprocessed through a filter and smoothers to reduce the interference of power frequency and impulse noise for a higher signal-to-interference ratio, named as characteristic signals R_1-R_8. Correspondingly, the sEMG signal can be used as a power signal from the point of view of signal analysis. The representative indexes including macro vector set and micro vector set can be calculated on each of the eight preprocessed signals of gestures, and then concatenated to form a multi-dimensional feature matrix. This feature matrix is provided to a non-linear discriminant analysis classifier. The specific construction of the method is as follows.

III. RESULTS AND DISCUSSION

A. SEMG SIGNAL PREPROCESSING ALGORITHM

The raw signal data for sEMG signals are nonlinear, tiny-amplitude bioelectrical signals generated when muscle tissue expands or contracts. The presence of some noise information in the signal is due to the stochastic variation of the signal, the effect of the acquisition environment, and the differences of individual experimenters. For continuous signals containing non-action parts, efficient segmentation should be performed first to obtain useful parts. In fact, since the intensity of muscle movement is proportional to the amplitude of the signal, the indicator of signal energy can reflect the period of finger activity. Accordingly, we can integrate the continuous signal data in a period of time in a square, and the integral formula is given by Eq. (1)

$$E_x = \int_{t_0}^{t_0+T} |S_x(t)|^2 dt = \sum |S_x(n)|^2 \qquad (1)$$

here, E is the signal energy for a period of time T, x is the energy value at a certain time T. S_x is the continuous signal,

and n is the length of the signal data. Furthermore, we used the sliding rectangular window (the width was set as θ, and the sliding step was set as $\theta/2$) to calculate the energy value. For improving the accuracy and reducing distractions, the starting threshold α and ending threshold β were set, respectively, which were adjustable depending on the actual collected data of different gestures. When the absolute value of E is greater than the absolute value of α in period of time T, the starting time of the first rectangular window can be used as the starting point of the action part of the signal. As opposed to this, when the absolute value of E is less than the absolute value of α in period of time T, the starting time of the first rectangular window can be used as the ending point of the action part of the signal. Therefore, the feature signals R_1-R_8 are converted into a pre-processed signal, named F_1-F_8, which can be used for pattern recognition in the next step.

B. CHARACTERISTIC VECTOR EXTRACTION ALGORITHM

As explained above, the sEMG signal can be considered as a power spectral density. In addition, the processed signal F_i(F_1-F_8) contains plenty of feature information corresponding to each gesture, which is necessary to be extracted. Therefore, six representative characteristic indexes, including the peak position (PP), mean absolute value (MAV), integral electromyogram (IEMG), peak value (PV), wave length (WL), and zero crossing (ZC), were calculated from the signal data F_i, and they were shown in Figure 2(b). Considering the complexity of EMG signals, including low frequencies, low values, and differences, the remaining signals should be of interest in feature extraction. In other words, it is necessary to pay close attention to the microscopic features lurking in the signal. However, PP characterizes the individual local locations of the signal, while IEMG, MAV, WL, and ZC characterize the macroscopic features of the time domain, which can all be considered as macroscopic features. Thereupon, wave-let packet analysis, which can provide a more refined decomposition scheme, was used to express the microscopic characteristics (contains time and frequency domain characteristics) lurking in the signals. Following closely, the structural information in the data can be extracted in a multiscale manner. According to the orthogonality and self-similarity principle, wavelet packet transform with 'dmey', was applied to decompose the data F into three layers (see Figure 3). The sequence of characteristic signal space domain can actually be mapped to the sequence of new space, called frequency bands, which is constructed by the basis function of wavelet packet through wavelet packet analysis [30], [31], [32]. Therefore, the signal processed by the wavelet packet analysis can be further extracted in micro space including both time and frequency domains. Accordingly, the signal energy Ej of frequency bands in the scale space can be set as a set of features for signal recognition, which was given by Eq. (2)

$$E_j = \int |S_j(t)|^2 dt = \sum_k |S_j(k)|^2 \tag{2}$$

where j (j = 1, 2, …, 8) is the number of frequency bands of signal energy, S_j(Figure 3(d)) is rebuilt from the power spectral density of each frequency band node, formed by wavelet packet decomposition, and k stands for data length. The stability of the feature index obtained by wavelet packet decomposition is very important for the accuracy of subsequent pattern recognition. Accordingly, we introduce the minimum entropy criterion to obtain the optimal subspace to ensure the stability of the feature index. Thus, the most stable state of information of the characteristic signal can be set as another important characteristic index, which can be calculated by the sum of the optimal subspace entropy (SOSE) as Eq. (3) shown. And the entropy can be calculated by Eq. (4).

$$SOSE = \sum E(s_t) = -\sum {s_t}^2 \log(s_t^2) \tag{3}$$

$$E(s_t) = -s_t^2 \log(s_t^2) \tag{4}$$

here, s_t is the coefficient of the signal F_i projecting onto an orthogonal wavelet basis of the optimal subspace. Accordingly, the local microscopic features and macroscopic features of the processed signal F_i, a total of 15 characteristic indexes (SOSE, IEMG, MAV, WL, ZC, PP, PV and E_1 to E_8), were extracted from each signal. Here, $SOSE_1$ ~$SOSE_n$ are the sum of the optimal subspace entropy of the signal F_1 ~F_n. $IEMG_1$ ~$IEMG_n$ are the integral electromyograms of the signal F_1 ~F_n. MAV_1 ~MAV_n are the mean absolute values of the signal F_1 ~F_n. WL_1 ~WL_n are the wave length of the signal F_1 ~F_n. ZC_1 ~ZC_n are the zero crossing of the signal F_1 ~F_n. PP_1 ~PP_n are the wave length of the signal F_1 ~F_n. PV_1 ~PV_n are the wave length of the signal F_1 ~F_n. [$E1_1$, $E1_n$]~[$E8_1$, $E8_n$] are the entropy of the signal F_1 ~F_n.

Thus, the characteristic vectors were constituted via the arrangement of indexes in a row generating the characteristic matrix MT (Eq. (5)), as shown at the bottom of the next page, which can characterize the flexion and extension of each finger.

C. CLUSTERING AND EXPERIMENTAL EVALUATION

To verify the ability of the developed rehabilitation system in the identification of different gestures for better passive training, the Hierarchical Cluster Analysis (HCA) and Principal Component Analysis (PCA) were adopted to cluster and classify the complex and high latitude data for self-recognition [33], [34]. As mentioned above, the characteristic indexes extracted from the signals of gestures can be formed as a high-latitude matrix M (15 indexes × 8 gestures × 5 replicates). HCA is used as a statistical method for multivariate variables on M, to explore the similarity among feature vectors. As shown in Figure 4, all eight kinds of signal samples corresponding gestures with 40 trials (The same gesture sample is repeated 5 times) were divided into eight branches at the total Euclidean distance 0.3 a.u.. In addition, the branches cluster into two groups at a total Euclidean distance of 2.7 a.u. and finally converge at a total Euclidean distance of 5.3 a.u. It can be seen that the groups

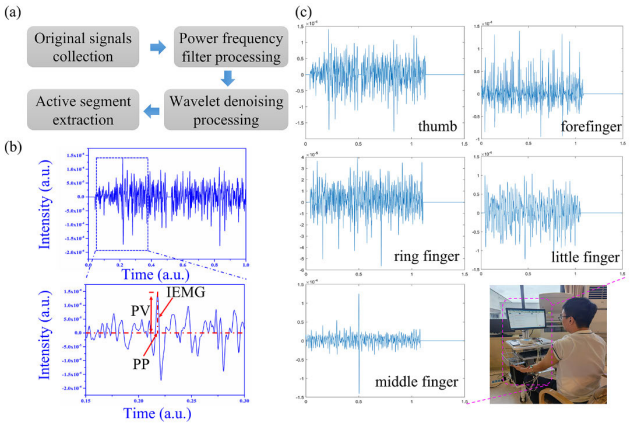

FIGURE 2. (a) Flow chart of signal processing, (b) the original signal and its partial enlarged view with conventional indexes, (c) the original signals of different gestures.

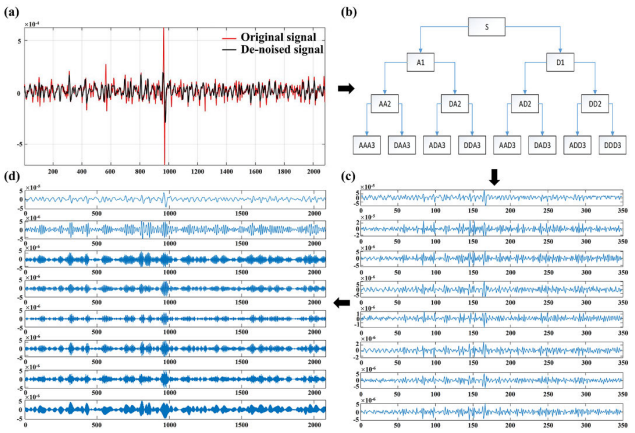

FIGURE 3. (a) The original EMG signals and its wavelet denoising result. (b) The three tree-based decomposition with dmey wavelet packet transform. (c) The wavelet coefficient of nodes at layer three. (d) The restructured signal for each node of the third frequency band.

represent the gesture signals in the two states (flexion and extension), respectively. Therefore, all samples can be accurately distinguished from each other without error in the HCA dendrogram.

In addition, PCA was applied to decrease the high dimensionality of the data matrix M through projecting the interconnected and complex dimensions onto new and independent dimensions, called components (PCs). From this, we obtain that the top 10 PCs occupy 92.34% of the total variance of the matrix, and the top 3 PCs occupy 44.59%, 23.17%, and 19.83%, respectively. The results are shown in Figure 5.

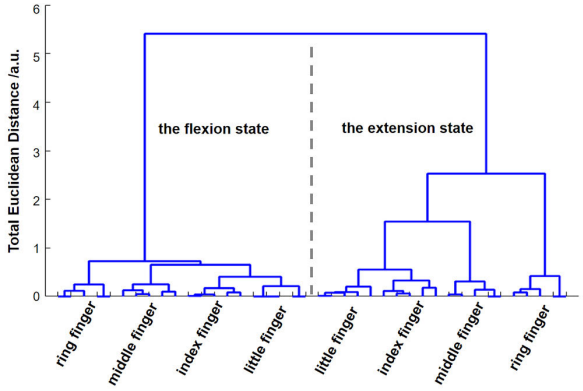

FIGURE 4. Hierarchical cluster analysis (HCA) for identification of eight kinds of gesture signals. All the samples were run in quintuplicate trials.

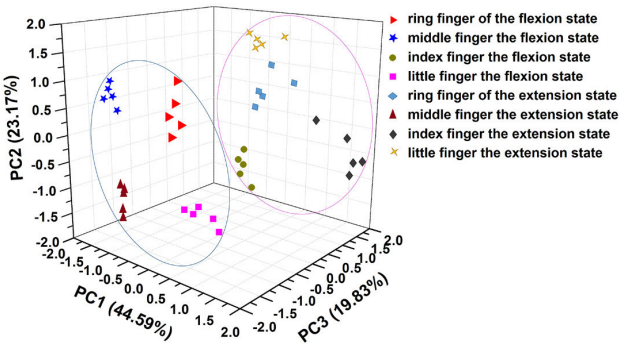

FIGURE 5. PCA three-dimensional score plot of 40 trials from eight kinds of gesture signals with excellent separation in the first three dimensions.

It turns out that the difference between gesture signals is not only related to the state of action, but also to the amount of muscle activity, the level of fatigue, and other indicators. Moreover, the distance between the same action state and gestures with different fatigue levels is shorter than the distance between different action states and gestures with distinct clustering phenomena, which is consistent with the HCA results.

IV. EXPERIMENTAL EVALUATION

A. REPEATABILITY AND ACCURACY OF THE RECOGNITION ALGORITHM

To evaluate the practical application of the proposed method for classification in signal samples. 40 samples from each finger at each state (flexion or extension) were detected by the

$$MT = \begin{bmatrix} SOSE_1 & IEMG_1 & MAV_1 & WL_1 & ZC_1 & PP_1 & E1_1 & \cdots & E8_1 & PV_1 \\ SOSE_2 & IEMG_2 & MAV_2 & WL_2 & IR_2 & PP_2 & E1_2 & \cdots & E8_2 & PV_2 \\ \vdots & \vdots & \vdots & \vdots & \vdots & \vdots & \vdots & \ddots & \vdots & \vdots \\ SOSE_n & IEMG_n & MAV_n & WL_n & IR_n & PP_n & E1_n & \cdots & E8_n & PV_n \end{bmatrix} = \left[MT_1^{\mathrm{T}}, MT_2^{\mathrm{T}}, \cdots, MT_n^{\mathrm{T}} \right]^{\mathrm{T}} \quad (5)$$

TABLE 1. The statistical results of recognition.

Kind	state	Selected number	Error of kind discrimination (number)
ring finger	flexion	34	1
	extension	35	0
middle finger	flexion	35	0
	extension	34	1
index finger	flexion	35	0
	extension	34	1
little finger	flexion	34	1
	extension	34	1

proposed method repeatedly with the male 28 and female 12. So, there were $40 \times 2 \times 4 = 320$ independent samples named 'A' in total. In the premise of each finger can be selected, 40 samples named 'B' were randomly selected (each kind of gesture signal were run in quintuplicate trials) from 'A' for recognition in accordance with the method based on PCA and HCA. As can be seen from Fig. 4, all the 40 samples 'B' can be accurately distinguished from each other without error in the HCA dendrogram. Furthermore, we also conducted experiments on the remaining 280 samples ('A' - 'B').

The table 1 shows that five samples are identified incorrectly with 98% accuracy. It indicates that the proposed method has a commendable repeatability and accuracy.

B. PASSIVE TRAINING CONTROL

In this mode, a stepper motor combined with a mechanical valve is applied as the main driver. The user adjusts the mechanical valve based on the trained finger joint. For instance, when the middle interphalangeal point and the distal inter-phalanx point need to be trained, the user can fix the mechanical valve with screws and further lock the synchronizing wheel |, so that the stepper motor can only train the specific finger joint. The mechanical valve can be loosened when the entire finger joint needs to be trained. Thus, after giving a certain angle, the stepper motor can drive the conveyor belt to train the entire finger joint. During training of the entire finger joint, the rehabilitation system can automatically control the motor for passive training in cooperation with the acquisition device and the proposed gesture recognition algorithm. Accordingly, passive training experiments were conducted (see Figure 6). Passive training is really to control the motor to work at a constant speed and to drive each joint to rotate. From a different perspective, the exoskeleton experiment is an angle experiment in which the exoskeleton drives the finger joints to rotate. Since the MCP of the exoskeleton is similar to that of the finger, we performed MCP angular rotation experiments on the index finger to verify the accuracy of the mechanical structure and recovery motion of the exoskeleton.

According to the MCP joint rotation experiment (Figure. S3), the maximum rotation angle can be obtained as 68.27°, according to the free flexion angle of human fingers

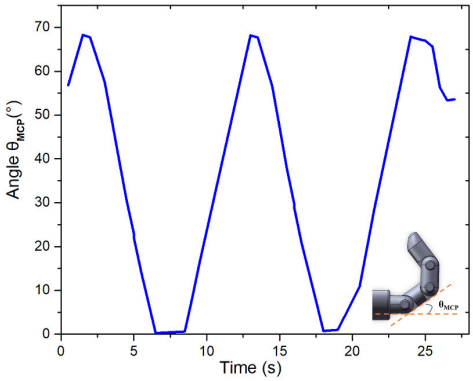

FIGURE 6. The change of MCP angle with training time.

as 70°, and the Angle error rate is 2.47%, which is less than 5%. Therefore, the exoskeleton designed in this paper can meet the requirements of rehabilitation training.

C. ACTIVE TRAINING CONTROL

In this mode, a damping axis with a leaf spring is employed as the resistance component, and the exoskeleton part of the recovery system is actuated by the fingers to perform flexion or extension actions while overcoming the resistance. The torque of the damping shaft can be regulated to provide a range of resistances to provide the patient with a requirement to gradually increase the intensity of the training of the finger muscles. The relation between the amount of deformation of the leaf spring and the torque is shown in Figure 7. Linear regression analysis indicates that the damping torque has a good linear relationship with the amount of deformation of leaf spring in the range from 0.1 mm to 14.5 mm. However, as the deformation of the leaf spring is further increased, the upward trend of the resistance increases exponentially. This is related to the coefficient of the leaf spring. At the same time, the maximum resistance reaches 26.7 N at 12.8 mm within the elastic range of the leaf spring. Generally, the fingers of patients with hand dysfunction or muscle damage can withstand a maximum force of 10 N, which is within the linear range provided by the damping device. From this, it is shown that the damping device employed here meets the intensity requirements of active training.

To assess the actual training effect and stability of this mode, four different levels of deformation, including 1mm, 2.5 mm, 4 mm, 5.5 mm were selected for analysis. Figure 8 shows that the forces measured by a thin film pressure sensor applied to the PIP during the finger bending. Distinctly, the force exerted on the PIP shows small fluctuations during the flexion motion, with mean values close to 3N and 6N for deformations of 1 mm and 2.5 mm, respectively. Nevertheless, when the deformation is larger than 3 mm, and in particular 5.5 mm, the force exerted on the PIP shows significant fluctuations with mean values of approximately 9N and 12N, respectively. This phenomenon is due to the shaking of the experimenter's fingers while grasping as the damping force is increased. From this, it can be concluded

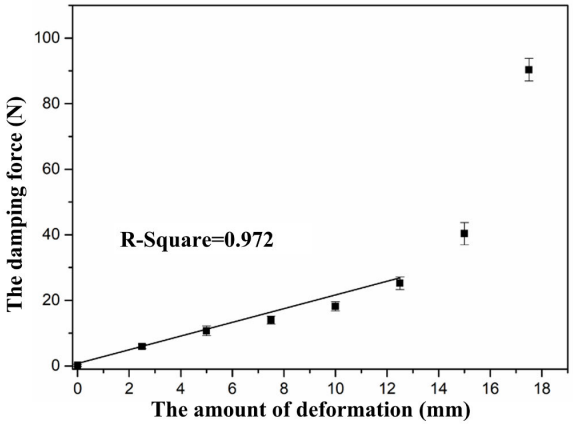

FIGURE 7. The relationship between the damping force and the amount of deformation. Error bars represented the standard deviations of three independent measurements.

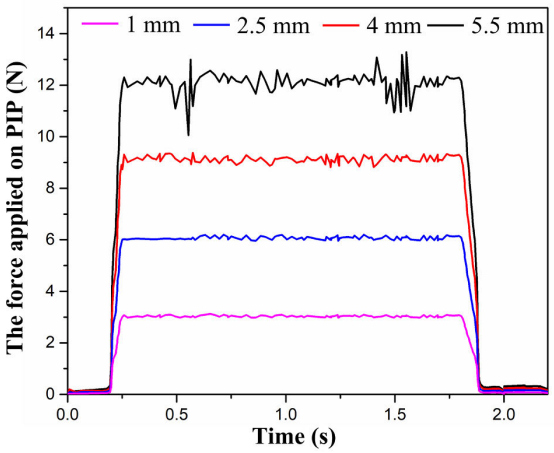

FIGURE 8. The force applied on PIP with different levels of deformation.

that the stability of the force exerted on the PIP gradually deteriorates as the amount of deformation increases. And the damping shaft with leaf spring used here can afford a stable damping resistance below 12N for finger grasping in active training mode.

V. CONCLUSION

In summary, a controllable, portable, effective hybrid-actuator exoskeleton was developed for finger rehabilitation applications. This system was powered by a direct-current motor for passive training and using the damping shafts with leaf springs to provide the damping force for active training. Compared to traditional passive training, real-time gesture intent recognition algorithm was proposed to automatically identify the bending state of different fingers for better training. Accordingly, the rehabilitation system exhibited good selectivity to the sEMG signals via extracting the characteristic vectors, including macroscopic features and microscopic features. To achieve independent training of each finger joint while making the system lightweight and structure simplified, an underactuated mechanism, which combines with the conveyor belt and a mechanical valve designed on the synchronizing wheel, can accurately transfer the driving to the finger joints. In addition, the damping force supplied by the damping shaft with leaf springs within the linear range is a stable active training mode. The damping force output with deformations below 4 mm can satisfy the intensity requirement of patients troubled by hand dysfunction or muscle damage. Thus, the proposed system with the novel gesture recognition method can be expected to be applied for finger rehabilitation training. With further optimization and upgrading, we believe that the rehabilitation system will have a potential practical value in rehabilitation facilities, communities, and home care.

REFERENCES

[1] S. Campagnini, P. Liuzzi, A. Mannini, R. Riener, and M. C. Carrozza, "Effects of control strategies on gait in robot-assisted post-stroke lower limb rehabilitation: A systematic review," *J. Neuroeng. Rehabil.*, vol. 19, no. 1, p. 52, Dec. 2022.

[2] N. Nordin, S. Xie, and B. Wünsche, "Assessment of movement quality in robot-assisted upper limb rehabilitation after stroke: A review," *J. Neuroeng. Rehabil.*, vol. 11, no. 1, p. 137, Sep. 2014.

[3] N. D. Armstrong, V. Srinivasasainagendra, A. Patki, R. M. Tanner, B. A. Hidalgo, H. K. Tiwari, N. A. Limdi, E. M. Lange, L. A. Lange, D. K. Arnett, and M. R. Irvin, "Genetic contributors of incident stroke in 10,700 African Americans with hypertension: A meta-analysis from the Genetics of Hypertension Associated Treatments and Reasons for Geographic and Racial Differences in Stroke studies," *Frontiers Genet.*, vol. 12, Dec. 2021, Art. no. 781451.

[4] S. Shafaq, J. Ings, E. Game, A. Wassef, M. Game, N. Rizvi, L. Malowany, and N. Dean, "Detection of masked hypertension among post-stroke patients," *Int. J. Stroke*, vol. 15, no. Supplement 1, p. 278, Nov. 2020.

[5] R. T. Pinzon and P. N. Nunsio, "OR69. The impact of hypertension on clinical outcome of hemorrhagic stroke patients," *Eur. Heart J. Supplements*, vol. 23, no. Supplement F, p. 68, Nov. 2021.

[6] A. Alloubani, R. Nimer, and R. Samara, "Relationship between hyperlipidemia, cardiovascular disease and stroke: A systematic review," *Current Cardiol. Rev.*, vol. 17, no. 6, Nov. 2021, Art. no. e051121189015.

[7] R. Menet, M. Bernard, and A. ElAli, "Hyperlipidemia in stroke pathobiology and therapy: Insights and perspectives," *Frontiers Physiol.*, vol. 9, p. 488, May 2018.

[8] N. Parnianfard, S.-R. Sadat-Ebrahimi, and P. Hoseini, "Hyperlipidemia as a stroke risk factor: Study of patients from Northwest of Iran from 2008 to 2013," *Atherosclerosis*, vol. 315, p. E196, Dec. 2020.

[9] S. H. Kim, D. E. Huizenga, I. Handzic, R. E. Ditwiler, M. Lazinski, T. Ramakrishnan, A. Bozeman, D. Z. Rose, and K. B. Reed, "Relearning functional and symmetric walking after stroke using a wearable device: A feasibility study," *J. Neuroeng. Rehabil.*, vol. 16, no. 1, p. 106, Dec. 2019.

[10] R. Joundi, G. Saposnik, R. Martino, J. M. Fang, V. Giannakeas, J. Porter, and M. Kapral, "Disability and mortality after permanent feeding tube placement in patients with acute stroke," *Neurology*, vol. 88, no. Supplement 16, p. 88, Apr. 2017.

[11] C. C. Carame, L. A. Pascasio, A. G. Pastor, A. M. I. Mohedano, F. D. Otero, P. V. Alen, M. V. Montero, Y. F. Bullido, S. P. Sanchez, M. M. Serrano, and A. C. G. Nunez, "Minor stroke can cause major disability: Identification of poor prognosis factors in patients with minor stroke," *J. Neurol. Sci.*, vol. 429, pp. 15–16, Oct. 2021.

[12] E. Amirpour, R. Fesharakifard, H. Ghafarirad, S. M. Rezaei, A. Saboukhi, M. Savabi, and M. R. Gorji, "A novel hand exoskeleton to enhance fingers motion for tele-operation of a robot gripper with force feedback," *Mechatronics*, vol. 81, Feb. 2022, Art. no. 102695.

[13] R. M. Viglialoro, S. Condino, G. Turini, V. Mamone, M. Carbone, V. Ferrari, G. Ghelarducci, M. Ferrari, and M. Gesi, "Interactive serious game for shoulder rehabilitation based on real-time hand tracking," *Technol. Health Care*, vol. 28, no. 4, pp. 403–414, Jul. 2020.

[14] L. T. Triccas, J. H. Burridge, A. M. Hughes, K. L. Meadmore, M. Donovan-Hall, J. C. Rothwell, and G. Verheyden, "A qualitative study exploring views and experiences of people with stroke undergoing transcranial direct current stimulation and upper limb robot therapy," *Topics Stroke Rehabil.*, vol. 25, no. 7, pp. 480–488, Oct. 2018.

[15] L. Li, Q. Fu, S. Tyson, N. Preston, and A. Weightman, "A scoping review of design requirements for a home-based upper limb rehabilitation robot for stroke," *Topics Stroke Rehabil.*, vol. 29, no. 6, pp. 449–463, Aug. 2022.
[16] C. Hernández-Santos, Y. A. Davizón, A. R. Said, R. Soto, L. C. Félix-Herrán, and A. Vargas-Martínez, "Development of a wearable finger exoskeleton for rehabilitation," *Appl. Sci.*, vol. 11, no. 9, p. 4145, May 2021.
[17] K. August, D. Bleichenbacher, and S. Adamovich, "Virtual reality physical therapy: A telerehabilitation tool for hand and finger movement exercise monitoring and motor skills analysis," in *Proc. 31st Annu. Northeast Bioeng. Conf.*, Apr. 2005, pp. 73–74.
[18] K. O. Thielbar, T. J. Lord, H. C. Fischer, E. C. Lazzaro, K. C. Barth, M. E. Stoykov, K. M. Triandafilou, and D. G. Kamper, "Training finger individuation with a mechatronic-virtual reality system leads to improved fine motor control post-stroke," *J. Neuroeng. Rehabil.*, vol. 11, no. 1, p. 171, Dec. 2014.
[19] L. Li, R. He, M. S. Soares, S. Savovic, X. Hu, C. Marques, R. Min, and X. Li, "Embedded FBG-based sensor for joint movement monitoring," *IEEE Sensors J.*, vol. 21, no. 23, pp. 26793–26798, Dec. 2021.
[20] M. R. Golomb, B. C. McDonald, S. J. Warden, J. Yonkman, A. J. Saykin, B. Shirley, M. Huber, B. Rabin, M. AbdelBaky, M. E. Nwosu, M. Barkat-Masih, and G. C. Burdea, "In-home virtual reality videogame telerehabilitation in adolescents with hemiplegic cerebral palsy," *Arch. Phys. Med. Rehabil.*, vol. 91, no. 1, pp. 1–8, Jan. 2010.
[21] A. A. Moshaii, M. M. Moghaddam, and V. D. Niestanak, "Fuzzy sliding mode control of a wearable rehabilitation robot for wrist and finger," *Ind. Robot*, vol. 46, no. 6, pp. 839–850, Nov. 2019.
[22] S. K. Manna and V. N. Dubey, "A portable elbow exoskeleton for three stages of rehabilitation," *J. Mech. Robot.*, vol. 11, no. 6, Dec. 2019, Art. no. 065002.
[23] S. Chiyohara, J.-I. Furukawa, T. Noda, J. Morimoto, and H. Imamizu, "Passive training with upper extremity exoskeleton robot affects proprioceptive acuity and performance of motor learning," *Sci. Rep.*, vol. 10, no. 1, p. 11820, Jul. 2020.
[24] M. Herde, D. Kottke, A. Calma, M. Bieshaar, S. Deist, and B. Sick, "Active sorting—An efficient training of a sorting robot with active learning techniques," in *Proc. IEEE IJCNN*, Jul. 2018, pp. 1–8.
[25] O. Sandoval-Gonzalez, J. Jacinto-Villegas, I. Herrera-Aguilar, O. Portillo-Rodiguez, P. Tripicchio, M. Hernandez-Ramos, A. Flores-Cuautle, and C. Avizzano, "Design and development of a hand exoskeleton robot for active and passive rehabilitation," *Int. J. Adv. Robotic Syst.*, vol. 13, no. 2, p. 66, Mar. 2016.
[26] R. S. Araujo, C. R. Silva, S. P. N. Netto, E. Morya, and F. L. Brasil, "Development of a low-cost EEG-controlled hand exoskeleton 3D printed on textiles," *Frontiers Neurosci.*, vol. 15, Jun. 2021, Art. no. 661569.
[27] T. Zhong, D. Li, J. Wang, J. Xu, Z. An, and Y. Zhu, "Fusion learning for sEMG recognition of multiple upper-limb rehabilitation movements," *Sensors*, vol. 21, no. 16, p. 5385, Aug. 2021.
[28] N. Nasri, S. Orts-Escolano, and M. Cazorla, "An sEMG-controlled 3D game for rehabilitation therapies: Real-time time hand gesture recognition using deep learning techniques," *Sensors*, vol. 20, no. 22, p. 6451, Nov. 2020.
[29] G. Yin, X. Zhang, and J. C. Chen, "An approach for sEMG-based variable damping control of lower limb rehabilitation robot," *Int. J. Robot. Autom.*, vol. 35, no. 3, pp. 171–180, 2020.
[30] E. Berthe, D.-M. Dang, and L. Ortiz-Gracia, "A Shannon wavelet method for pricing foreign exchange options under the Heston multi-factor CIR model," *Appl. Numer. Math.*, vol. 136, pp. 1–22, Feb. 2019.
[31] X. Sui, K. Wan, and Y. Zhang, "Pattern recognition of sEMG based on wavelet packet transform and improved SVM," *Optik*, vol. 176, pp. 228–235, Jan. 2019.
[32] S. Choe and J. Yoo, "Wavelet packet transform modulus-based feature detection of stochastic power quality disturbance signals," *Appl. Sci.*, vol. 11, no. 6, p. 2825, Mar. 2021.
[33] M. N. M. Asri, W. N. S. M. Desa, and D. Ismail, "Combined Principal Component Analysis (PCA) and Hierarchical Cluster Analysis (HCA): An efficient chemometric approach in aged gel inks discrimination," *Austral. J. Forensic Sci.*, vol. 52, no. 1, pp. 38–59, Jan. 2020.
[34] M. Szczepanik, J. Szyszlak-Bargłowicz, G. Zając, A. Koniuszy, M. Hawrot-Paw, and A. Wolak, "The use of multivariate data analysis (HCA and PCA) to characterize ashes from biomass combustion," *Energies*, vol. 14, no. 21, p. 6887, Oct. 2021.

SHIXIAN ZHAO was born in Henan, China, in 1990. He received the M.E. and Ph.D. degrees in biomedical engineering from Chongqing University, Chongqing, China, in 2016 and 2019, respectively.

He is currently an Associate Professor with the Chongqing Engineering and Technology Research Center of Intelligent Rehabilitation and Eldercare. His research interests include robot techniques and theories and their applications in rehabilitation engineering.

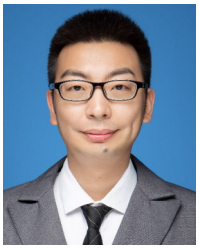

JINCAN LEI was born in Chongqing, China, in 1983. He received the B.E. degree in biomedical engineering from the University of Shanghai for Science and Technology, Shanghai, China, in 2007, and the M.E. and Ph.D. degrees in biomedical engineering from Chongqing University, Chongqing, in 2010 and 2014, respectively.

He is currently an Associate Professor with the Chongqing Engineering and Technology Research Center of Intelligent Rehabilitation and Eldercare. His research interests include algorithm design, modeling and simulation, and rehabilitation engineering theories.

QIHENG TIAN is currently a Professor with the Chongqing Engineering and Technology Research Center of Intelligent Rehabilitation and Eldercare. He is a Chief Expert of the Collaborative Innovation Team. His research interests include theories of geriatric rehabilitation medicine and limb prostheses.

ZHIHAO YANG was born in Sichuan, China, in 1995. He received the B.E. and M.E. degrees in biomedical engineering from Chongqing University, Chongqing, China, in 2020 and 2022, respectively, where he is currently pursuing the Ph.D. degree with the Key Laboratory for Biorheological Science and Technology of Ministry of Education.

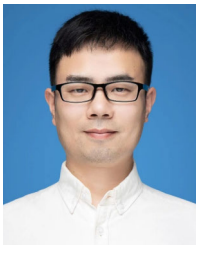

JING HUANG was born in Hunan, China, in 1983. He received the B.E. and Ph.D. degrees in biomedical engineering from Chongqing University, Chongqing, China, in 2007 and 2017, respectively.

His research interests include motor drive control, algorithm design, and rehabilitation engineering theories.